Ni(II) METAL CHELATES WITH 2-(2-THIAZOLYLAZO)-4-METHOXYPHENOL IN SOLUTION — A COMBINED GRAPHICAL AND NUMERICAL INTERPRETATION OF ABSORBANCE CURVES*

V.KUBÁŇ[a], L.SOMMER[a] and J.HAVEL[b]**

[a] *Department of Analytical Chemistry, J. E. Purkyně University, 611 37 Brno and*
[b] *Department of Inorganic Chemistry, Royal Institute of Technology, S-100 44, Stockholm 70, Sweden*

Received April 23rd, 1974

Complexes with compositions NiL^+, NiL_2, $NiLH^{2+}$ and NiL_2H^+ ($\log \beta_{11} = 7{\cdot}59_5$, λ_{max} 609 nm, ε_{max} 16260; $\log \beta_{12} = 15{\cdot}81_5$, λ_{max} 625 nm, ε_{max} 33320) are formed in Ni(II) solutions containing 2-(2-thiazolylazo)-4-methoxyphenol (TAMP) and 30% vol. ethanol, under various experimental conditions. Combination of graphical data analysis with numerical treatment of absorbance curves using the PRCEK and LETAGROP SPEFO programs has proven very effective for the determination of the complex characteristics. The results obtained using the three methods are in very good agreement. As a potential basis for the spectrophotometric determination of nickel with TAMP, only the ML_2 complex can be considered (λ_{max} 625, ε_{max} 33320), which is formed in solutions containing excess ligand, $c_L/c_M > 15$, at pH $\geqq$ 6·5.

In the large group of heterocyclic azo-dyes based on thiazole, 2-(2-thiazolylazo)-4-methoxyphenol (abbreviated below as TAMP) and its derivatives have proven advantageous as very sensitive metallochromic indicators in chelometric titrations and as suitable reagents for the spectrophotometric determination of many metal ions[1-14]. The formation of coloured chelates is accompanied by large colour contrasts ($\Delta\lambda = \lambda_{max}^{ML} - \lambda_{max}^{L}$) typical for N-heterocyclic azo-dyes substituted in the *p*-position with respect to the phenolic hydroxyl. The acid–base properties of TAMP were studied several times in various mixed media and in water; data on its optical and acid–base properties in various media are summarized in a paper by Kubáň and Havel[14].

In the present paper, complexation equilibria of nickel(II) ions with TAMP are studied spectrophotometrically in a medium of 30% ethanol. The results of the graphical and graphical-logarithmic analysis of the absorbance curves using slope-intercept transformations[15-18] were compared with the results of the data treatment by the linear least squares method using the PRCEK type programs[19,20] and with the results obtained by a universal minimizing program, LETAGROP SPEFO[21,22],

* Part II in the series Some 2-(2-Thiazolylazo)-4-methoxyphenol (TAMP) Complex Equilibria; Part I: Acta Chem. Scand. *27*, 528 (1973).

** Present address: Department of Analytical Chemistry, J. E. Purkyně University, 611 37 Brno.

which has been used during interpretation of data for the TAMP acid–base equilibria[14]. Calculation of distribution diagrams according to the HALTAFALL program[23–25] from the final equilibrium constant values enabled accurate assessment of the distribution of individual complexes under various experimental conditions.

EXPERIMENTAL

Chemicals and solutions. 2-(2-Thiazolylazo)-4-methoxyphenol (TAMP) was prepared by Svoboda and Bendová[26]. The commercial substance was recrystallized twice from hot ethanol and dried over P_2O_5 in a dessicator. The content of the dye active component was determined by elemental analysis for C, H and N and from the content of the sulphate ash. The substance purity was tested by thin-layer chromatography on the MN-Kieselgel G silica from the firm, Macheray-Nagel[27]. A TAMP stock solution (c_R — $5 . 10^{-4}$ — $5 . 10^{-3}$M) was prepared by dissolving the crystalline substance in 2·5 ml dimethylformamide and 2·5 ml 1M-NaOH or 1M-NH_4OH at laboratory temperature and diluting to the required amount with water or ethanol. The resulting DMF concentration in the stock solution was always less than 1% v/v and in the measured solutions varied within 0·1—0·2% v/v. A nickel(II) ion standard solution was prepared from recrystallized $Ni(NO_3)_2$ *p.a.*, by dissolving it in 0·1M-HNO_3; it was standardized gravimetrically or by EDTA titration with murexide indicator. The stock solutions were diluted with 0·1M-HNO_3. The ionic strength of the solutions was maintained constant at a value of $I = 0{\cdot}10$ with twice recrystallized KNO_3 or with a mixture of HNO_3, KNO_3 and NaOH. All other chemicals and solvents were commercial *p.a.* products, purified by recrystallization, distillation *etc.* The ethanol used contained 5% v/v methanol.

Instruments. Absorption spectra of solutions were measured on the Unicam SP 700 recording spectrophotometer at a temperature of 20°C. The solution acidity was measured with the PHM-4d pH-meter (Radiometer, Copenhagen) with a precision of ±0·02 pH unit, using the G 202 B glass and K 401 saturated calomel electrodes. The pH values in the mixed medium were not corrected and the symbol pH was used for them. Other spectrophotometric measurements were performed with the SFD-2 single-beam spectrophotometer in 5—20 mm cuvettes, at a constant

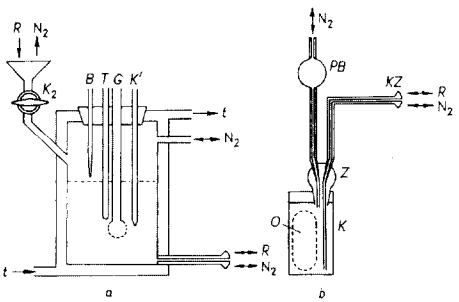

FIG. 1

Scheme of the Titration Vessel (*a*) and the Modified Photometer Cuvette (*b*)

R Solution, N_2 stream of inert gas, *K2* stopcock, *B* burettes, *T* thermometer, *G* glass electrode, *K* calomel electrode, t inlet and outlet of tempering water of the *U* 10 ultrathermostat, *K* photometer cuvette, *O* window in the cuvette holder, *PB* safety trap, *KZ* spherical ground-glass joint, *Z* cuvette ground-glass joint.

temperature of $t = 25{\cdot}00 \pm 0{\cdot}05°C$ in a nitrogen atmosphere, using a special apparatus; the procedures employed are described with individual experimental dependences.

The instrument for spectrophotometric measurements in a nitrogen atmosphere and in a closed cycle. A 200 ml double-mantle thermostatted cell (Fig. 1*a*) was used as a titration vessel. The solution temperature was maintained constant with the U 10 ultrathermostat (Medizinische Geräte, GDR). The ambient temperature was also maintained constant at $t = 25{\cdot}0 \pm 0{\cdot}1°C$.

The titration vessel was connected with the photometer cuvette through thick-walled capillaries, interconnected by two ball ground-glass joints, so that the system was sufficiently mobile during manipulations with the cuvette holder of the SFD-2 spectrophotometer (USSR).

A cuvette with a larger front area and a ground-glass joint, which is a part of the SP 525 Autocell Accessory (Unicam, England), was closed with a ground-glass stopper with two glass capillaries (Fig. 1*b*). One of the capillaries was connected to the titration vessel through a thick-walled capillary with a ball ground-glass joint and the other was connected, using a four-way stopcock, either to a nitrogen cylinder or with the atmosphere. A block scheme of the apparatus[28] is shown in Fig. 2.

The preparation of solutions with various parameters (pH, c_M, c_L or x_L) was carried out in the titration vessel by titration with solutions with various values of the given parameter. After establishment of equilibrium in the vessel, the pH of solution was measured and the solution was transported from the titration vessel into the photometer cuvette by overpressure of the inert gas. The cuvette was rinsed several times with the solution from the titration vessel, the absorbance values were measured after balancing the levels in the two parts of the apparatus and the solution was transferred back into the vessel by the inert gas overpressure. The solution acidity was measured again. The value of the variable parameter was changed again by adding solutions from burettes and the whole procedure was repeated with a new solution.

The parameters can be varied by arbitrary steps in measuring individual spectrophotometric dependences, using some of the procedures described later.

Graphical Interpretation of the Data

The graphical and graphical-logarithmic analysis of the curves of absorbance dependences on the component concentrations and on the solution acidity have already been described[14–18]. Here, only the resulting forms of the relations for A, c_M/A or c_L/A are given, along with the logarithmic transformations of the equations for the equilibrium or conditional stability constants of the assumed complexation

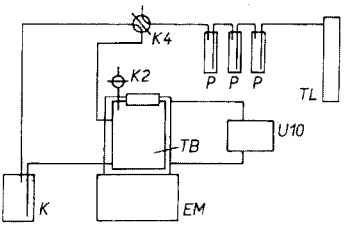

FIG. 2

Block Scheme of the Apparatus for Spectrophotometric Measurements in a Nitrogen Atmosphere

TL Inert gas cylinder, *P* column with the BTS catalyst and a set of traps containing NaOH, H_2SO_4 and the medium used, *U 10* the *U* 10 ultrathermostat, *K2* and *K4* two- and four-way stopcock, respectively, *TB* titration vessel, *EM* electromagnetic stirrer, *K* photometer cuvette.

equilibrium in solutions with excess ligand or excess metal ion or for equimolar solutions. Appropriate equations for the general equilibrium

$$m\,\mathrm{M} + n\,\mathrm{LH_x} \rightleftarrows \mathrm{M_mL_nH_{nx-q}} + q\,\mathrm{H}\,, \qquad (A)$$

$$K_{mqn} = [\mathrm{M_mL_nH_{nx-q}}]\,[\mathrm{H}]^q/[\mathrm{M}]^m\,[\mathrm{LH}]^n$$

and for some particular cases and concentration ratios are given in Table I.

TABLE I

The Equations for the Direct and Logarithmic Graphical Analysis of the Absorbance Curves and the Equations for the PRCEK II Program

Conditions	Y_i	Functions F_i, G_i	
$c_M \ll c_L$	$A - A_{OM}$	$\varepsilon_1 c_L + (\varepsilon_2 c_L - nA)^n\, c_M^m K/h^q\,.$ $.\,(\varepsilon_2 - n\varepsilon_1)^{n-1}$	$A_{01} + F_i K$
	$A - A_{OM}$	$\varepsilon_2 c_L + (\varepsilon_1 c_L - A)\, h^q/(\varepsilon_2 c_L - nA)^{n-1}\,.$ $.\,c_M^m K(\varepsilon_2 - n\varepsilon_1)^{1-n}$	$A_{02} +$ $+ G_i K^{-1}$
	$\log (A - A_{01})/(A_{02} - A)^n$	$\log K + q\ \mathrm{pH} + m \log c_M - (n-1)$ $\log (\varepsilon_2 - n\varepsilon_1)$	
$c_L \ll c_M$	$A - A_{OL}$	$\varepsilon_1 c_M + (\varepsilon_2 c_M - mA)^m\, c_L^n K/h^q\,.$ $.\,(\varepsilon_2 - m\varepsilon_1)^{m-1}$	$A_{01} + F_i K$
	$A - A_{OL}$	$\varepsilon_2 c_M + (\varepsilon_1 c_M - A)\, h^q/(\varepsilon_2 c_M -$ $-mA)^{m-1}\, c_L^n K(\varepsilon_2 - m\varepsilon_1)^{1-m}$	$A_{02} +$ $+ G_i K^{-1}$
	$\log (A - A_{01})/(A_{02} - A)^m$	$\log K + q\ \mathrm{pH} + n \log c_L - (m-1)$ $\log (\varepsilon_2 - m\varepsilon_1)$	
$c_M = c_L$	$A - A_{OM}$	$\varepsilon_1 c_L + (\varepsilon_2 c_L - nA)^{2n}\,.$ $.\,(\varepsilon_2 - n\varepsilon_1)^{2n-1}\, K/h^q$	$A_{01} + F_i K$
$m = n$	$A - A_{OM}$	$\varepsilon_2 c_L + [(A - \varepsilon_1 c_L)\,.$ $.\,(\varepsilon_2 - n\varepsilon_1)^{2n-1}\, h^q/K]^{1/n}$	$A_{02} +$ $+ G_i K^{-1}$
	$\log (A - A_{01})/(A_{02} - A)^{2n}$	$\log K + q\ \mathrm{pH} - (2n-1)$ $\log (\varepsilon_2 - n\varepsilon_1)$	
$c_M \simeq c_L$ [a]	$A - A_{OM}$	$\varepsilon_1 c_L + (c_L - n\,\Delta A/\Delta\varepsilon)^n\,.$ $.\,(c_M - m\,\Delta A/\Delta\varepsilon)^m\, K/h^q$	$A_{01} + F_i K$
	$mA - (nc_M - mc_L)\,\varepsilon_1$	$\varepsilon_2 c_L - \Delta A h^q/(c_L - n\,\Delta A/\Delta\varepsilon)^n\,.$ $.\,(c_M - m\,\Delta A/\Delta\varepsilon)^{m-1}\, K$	$A_{02} +$ $+ G_i K^{-1}$
	$\log (\Delta A/\Delta\varepsilon)/(c_L - n\,\Delta A/\Delta\varepsilon)^n\,.$ $.\,(c_M - m\,\Delta A/\Delta\varepsilon)^m$	$\log K + q\ \mathrm{pH}$	

[a] $\Delta A = A - c_M\varepsilon_M - c_L\varepsilon_1$; $\Delta\varepsilon = \varepsilon_2 - n\varepsilon_1 - m\varepsilon_M$; $A_{01} = \varepsilon_1 c_L$ or $\varepsilon_1 c_M$; $A_{02} = \varepsilon_2 c_L$ or $\varepsilon_2 c_M$.

Assuming that a single complexation equilibrium is established in solution, the dependences $A = f(F_i)$ or $A = f(G_i)$, or the corresponding dependences c_M/A or c_L/A, are linear only for correct values of the molar reaction coefficients, m, q and n in general equilibrium (A). The parameters of a straight line thus determine the reaction mechanism, the complex stoichiometry, the molar absorption coefficient (the intercept on the y-axis) and the equilibrium or conditional stability constant (the slope of the straight line). The equilibrium constant of the reaction, K_{mqn}, and the reaction mechanism were also verified using related plots of $\log F = f(\mathrm{pH})$, $\log F = f(\log c_M)$ or $\log F = f(\log c_L)$, as the intercept value $(\log K)$ and the slope (q) of the dependence.

A_{01} and A_{02}, as the absorbances calculated directly from the two horizontal parts of the absorbance *vs* acidity or absorbance *vs* component concentration curves were used as initial values for calculation. If some of the horizontal parts were not experimentally accessible, the A_{01} or A_{02} value was assessed by successive approximations. More accurate values of absorbances A_{01} or A_{02} were then obtained by graphical extrapolation of not entirely linear parts of the dependences and the thus-obtained values were used as initial values of the two quantities in another computing cycle; the process was repeated until the required degree of agreement between two successive values if A_{01} or A_{02} was achieved.

The successive approximation method was also used for examining equilibria in solutions with a small excess concentration of one component, when the values to be determined, A_{0i}, or the corresponding values of ε_i, also appear in the expressions for F_i or G_i. The above equations also hold for transition between two complexes, if the free concentration of the minor component can be neglected; if correction factors for ligand dissociation or cation hydrolysis are introduced, the equations are also valid for examining complexation equilibria with simultaneous dissociation of the ligand or hydrolysis of the cation in the studied acidity range[16].

If an extensive set of absorbance–pH curves are analyzed at a constant concentration of one component and varying concentration of the other in excess, then for the pH_{0i} values, corresponding to the same particular absorbance values A_i on the individual curves (corresponding solutions), the relation between pH_{0i} and the logarithmus of the variable concentration of the excess component is given by

$$\mathrm{pH}_{0i} = -(m/q) \cdot \log (c_M) + \text{const.}, \qquad (1)$$

$$\mathrm{pH}_{0i} = -(n/q) \cdot \log (c_L) + \text{const.} \qquad (2)$$

For solutions with variable concentration of the minor component, the following relations hold

$$\mathrm{pH}_{0i} = (m - 1)/q \cdot \log (c_M) + \text{const.}, \qquad (3)$$

$$\mathrm{pH}_{0i} = (n - 1)/q \cdot \log (c_L) + \text{const.} \qquad (4)$$

Similar equations can be derived for corresponding solutions with a series of curves of the absorbance *vs* the concentration of one component at a constant pH. If the excess concentration of the major component is small only a correction factor for the concentration bound in the complex is introduced.

The slope of the linear dependence of $pH_{0i} = f(\log c_M)$ or $pH_{0i} = f(\log c_L)$ estimates independently determines the ratio of the bound component and the number of protons being liberated, so that, when coefficient q is known, ambiguous situations can be avoided or the presence of a higher complex can be verified.

The same transformations as in the graphical and graphical logarithmic analysis of the absorbance–pH curves were also used for the interpretation of curves of the absorbance dependence on variable component concentration at a constant concentration of the other component and constant pH, where the presence of higher complexes, ML_n or M_mL, was verified independently. In this case the pH value appeared among the constant quantities and the concentration of one component was the variable.

Similarly as during the graphical analysis of absorbance curves, the basic equations for the overall solution absorbance, the overall component concentrations and the equilibrium or conditional reaction constant can be rearranged to obtain equations of straight lines, which have the following form for complex $M_mL_nH_{nx-q}$, equilibrium (A) and for the absorbance dependences on the metal or ligand concentration

$$c_M^{-m} = \text{const.}\ \Delta A^{-1} + \text{const.}\,, \tag{5}$$

$$c_L^{-n} = \text{const.}\ \Delta A^{-1} + \text{const.} \tag{6}$$

If the accurate component concentrations are not known, the c_M or c_L values can be replaced by the volumes of the solution added, v_M or v_L, respectively (refs[16,29,30]). The dependence is again linear if correct stoichiometric indexes m or n are introduced.

The above simple relations were used only for the determination of complex stoichiometry (the m and n values), while the molar absorption coefficients and equilibrium constants were not evaluated from their slope and intercept, because of poor precision (*i.e.* the two constant expressions in equations (5) and (6) include, in addition to quantities which are really constant, such as the concentration of one component, pH, ε_i, *etc.*, also higher terms of a binomial series[16]).

The method of continuous variations[31–33] was used under selected experimental conditions for the verification of the complex stoichiometry. In solutions of a constant ionic strength and in the absence of buffers, short absorbance-pH curves were measured for given mole fraction values, $x_L = c_L/(c_L + c_M)$, at several wavelengths and the absorbance values for a given pH were obtained by interpolation[17,18]. The thus-

-obtained absorbances were then corrected for the actual absorbance of the ligand and dependences $Y = A - A_L = f(x_L)$ were plotted.

Numerical Data Analysis Using the Linear Least Squares Method (the PRCEK type program)

During data handling by PRCEK type programs, the basic complex parameters, molar absorption coefficients, equilibrium constants and stoichiometry are determined analogously to the procedure followed during the graphical and graphical-logarithmic analysis of absorbance curves[19,20,28]. However, the parameters are determined objectively by the least squares method with repeated successive approximations.

As the first assessment of absorbances A_{01} and A_{02} or of ε_1 and ε_2, the values of the horizontal parts of the experimental absorbance–pH curves, $A = f(\text{pH})$ or of the concentration dependence curves, $A = f(c_{comp})$ were used. The molar absorption coefficient values of the free metal ion and of individual ligand acid–base species and the related dissociation constants were taken from the results of separate measurements and substituted into the expressions for F_i and G_i terms in the corresponding slope-intercept transformation relations. On the basis of these initial absorbance assessments and known values of ε_i, "better" values of absorbances A_{01} and A_{02} and of the equilibrium constant were successively determined and were then used in the following computation cycle as starting values for the calculation of terms F_i and G_i. The computation was repeated until the required agreement or precision between two successive values of absorbances A_{01} and A_{02} was achieved (the tolerance employed was $\Delta A \leqq 0{\cdot}002$ absorbance unit) or until the required number of approximations was reached (NI = 6).

After fulfilling these conditions, theoretical absorbances A_{calc} for individual points of the absorbance–pH curve, the sum of the squares of the deviations and the standard deviations of the molar absorption coefficients and the equilibrium constants were calculated from the "best" values of the two particles A_{01} and A_{02}, and of the reaction equilibrium constant. Using these absorbance values, the number of protons liberated during complexation or the number of coordinated particles of a given component were determined by logarithmic analysis, employing equations in the form, $\log F = f(\text{pH})$ or $\log F = f(\log c_M \text{ or } c_L)$.

These operations were carried out for each of the selected wavelengths separately and the resulting values of the reaction equilibrium constant and its logarithm were calculated, together with the appropriate standard deviations, as the average of the values for individual wavelengths.

For selecting the best combination of molar coefficients m, n and q in general equilibrium A, the correlation coefficient r_{xy} and the sum of the squares of deviations U were used as criteria both in direct and logarithmic analysis. In this case the

computation was always performed in a single cycle, usually only for the absorption maximum wavelength of the complex studied, and the tested combinations of molar reaction coefficients m, n and q were consecutively fed from the input medium. The combination of coefficients yielding the highest value of the correlation coefficient, r_{xy}, and the lowest sum of the squares of deviations U was then considered the most correct and further computation was performed with this combination.

Experimental absorbance values close to the limiting A_{01} or A_{02} values usually cause non-linearity of $A = f(F_i)$ or $A = f(G_i)$ plots, since minute experimental errors in absorbances lead to large deviations in the F_i and G_i values. Therefore, 10–20% of the points, for which it holds that $|A - A_{01}|$ or $|A_{02} - A| \leqq 0{\cdot}1 - 0{\cdot}2\,|A_{02} - A_{01}|$, were excluded from the program. Similarly, 20% of the points in both limiting regions in the logarithmic analysis were also omitted, so that the results were always obtained from c. 80% or 60% of the experimental values.

Data Interpretation Using the LETAGROP SPEFO Program

The absorbance–pH curves, $A = f(\mathrm{pH})$, and absorbance–concentration curves, $A = f(c_M, c_L)$, were also handled using a general minimization program, LETAGROP SPEFO[21,22] using the IBM 360/70 computer.

The program looks for the best combination of equilibrium constants $K_1, K_2, \ldots, K_N$ and molar absorption coefficients $\varepsilon_1, \varepsilon_2, \ldots, \varepsilon_N$ for wavelengths $\lambda_1, \lambda_2, \ldots, \lambda_N$ and for a given set of complexes in solution under given experimental conditions, yielding the minimum sum of the squares of the deviations of experimentally measured absorbances A_{exp} from the theoretical A_{calc} values, calculated from the equilibrium constants and molar absorption coefficients, using the general formula $A = \sum \varepsilon_{mqn} \cdot K_{mqn}[M]^m [LH_x]^n [H]^{-q}$. The sum of the squares of deviations U is then defined by

$$U = \sum_{1}^{NP} \sum_{1}^{NL} (A_{calc} - A_{exp})^2 , \qquad (7)$$

where NP and NL are the total number of points and of wavelengths, respectively. The computer automatically monitors the effect of individual newly considered complexes on the agreement of the experimental and theoretical absorbances (the sum of deviations) and the new complex is accepted as actually existing, or a complex accepted earlier is retained, only when the following condition is met for its equilibrium constant, K_i and the appropriate standard deviation, $\sigma(K_i)$

$$K_i \geqq F_\sigma \cdot \sigma(K_i) ,$$

where F_σ is a rejection factor. Its value can be chosen as required; in the present paper F_σ 1·5 has been chosen, corresponding to 93·3% probability.

In contrast to common practice during graphical data handling or during use of PRCEK type programs, for which the experimental conditions are chosen so that a single complex predominates in the solution (a large excess of one component, suitable acidity conditions, *etc.*), with the LETAGROP SPEFO program it is advantageous to select the experimental conditions so that the percentages of data are similar for all assumed complexes. This can be achieved either by selection of broad concentration and acidity intervals or by using data for solutions with small concentration excesses of the components.

Calculation of Distribution Diagrams Using the HALTAFALL Program

The distribution curves of the individual species in solution were calculated for some selected experimental conditions from the known values of the equilibrium constants and the complex stoichiometry[23-25], in dependence on the acidity and the component concentration ratios. The HALTAFALL program was employed and was translated into the Slang algoritmic language for the Minsk 22 computer[25], since its Algol[23] or Fortran[24] versions could not be directly applied.

RESULTS

Acid–Base Properties of the Ligand

In aqueous media and in mixed solutions containing ethanol, methanol or dimethylformamide, the orange-red cationic ligand form, LH_2^+ ($\lambda_{max} = 495-520$ nm, $\varepsilon_{max} \sim$

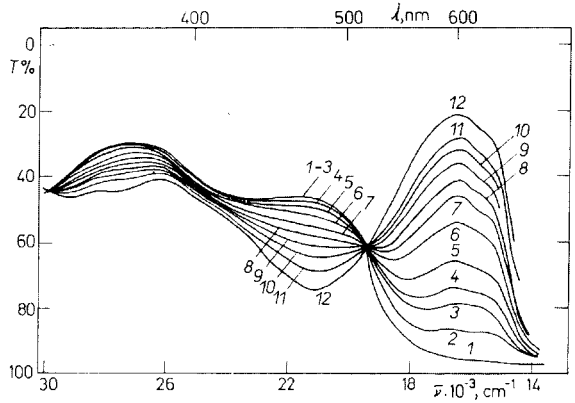

FIG. 3

Spectra of Ni(II)–TAMP Solutions in 30% Ethanol

$c_M = 100\, c_L = 4{\cdot}952 \,.\, 10^{-3}$M, $I = 0{\cdot}10$, t 25·00°C, d 10 mm. Curve, pH: *1* 1·12, *2* 1·41, *3* 1·78, *4* 2·05, *5* 2·20, *6* 2·36, *7* 2·60, *8* 2·76, *9* 2·90, *10* 3·10, *11* 3·22, *12* 3·62.

$\sim 10-11 \cdot 10^3$) predominates in strongly acid media at pH < 0, the orange-yellow molecular form, LH ($\lambda_{max} = 465-475$ nm, $\varepsilon_{max} \sim 7-10 \cdot 10^3$), at pH = 1–8 and, finally, the blue-purple anionic form, L^- ($\lambda_{max} = 560-570$ nm, $\varepsilon_{max} \sim 15-17 \cdot 10^3$), at pH > 9. The TAMP dissociation constants for LH_2^+/LH and LH/L^- transfers have been determined for various mixed media and water; here only the values for 30% ethanol are given ($pK_{a1} = 0{\cdot}12 \pm 0{\cdot}05$, $pK_{a2} = 8{\cdot}328 \pm 0{\cdot}017$), obtained from the ligand absorbance *vs* pH curves. Detailed information and the values for other media have already been published[14].

Complexation Equilibria of Ni(II) *with* TAMP

Spectra. The spectra of the Ni(II) reaction product with TAMP were measured in a medium containing 30% vol. ethanol in a pH interval from 1 to 8, for several c_M/c_L concentration ratios. In solutions with excess Ni^{2+}, the absorption maximum of the ligand molecular form (470 nm) disappears in dependence on the acidity and a double band appears for the chelate with a maximum of $\lambda_{max} = 609 \pm 3$ nm. The other absorption band of the ligand molecular form, LH, with maximum at 370 nm, is perceptibly split into two absorption bands with maxima at 356 and 383 nm (Fig. 3).

Two sharp isosbestic points at 332 and 518 nm indicate the simple transition of the ligand molecular form, LH, into the blue TAMP chelate with nickel in the studied pH range. The spectra exhibit a similar dependence on the concentration excess of Ni^{2+} at a constant solution pH.

TABLE II

The Optical Characteristics of the Complex Species in the Ni(II)–TAMP System $c_M = p_M \cdot c_L$, $t = 25{\cdot}00°C$, $I = 0{\cdot}10$, 30%ethanol.

c_M/c_L; pH[a]	$10^{-3}\,\nu_{max1}$ cm^{-1}		$10^{-3}\,\nu_{max2}$ cm^{-1}		λ_{max1}, nm		λ_{max2}, nm		$10^{-3}\,\nu_{i.p.}$ cm^{-1}		$\lambda_{i.p.}$, nm	
100[c]	28·1	26·1	16·4	15·5	356	383	611	650	30·1	19·3	332	518
10[c]	28·1	26·1	16·5	15·5	356	383	609	650	30·1	19·3	332	519
1[b]	27·5	26·0	16·4	15·5	364	385	609	647	30·2	19·2	330	523
1/4[b]	—	—	16·0	15·5	—	—	625	650	—	19·2	—	520
1/10[b]	—	—	16·0	15·5	—	—	625	650	—	19·3	—	518
3·55[a]	27·6	26·0	16·4	15·5	365	385	607	650	30·2	19·3	330	518
4·50[a]	27·9	26·1	16·4	15·5	359	385	607	650	30·2	19·2	330	520

[a] The spectra in dependence on the excess metal ion concentration at a constant solution acidity; [b] $c_M = 2{\cdot}476 \cdot 10^{-5}$M; [c] $c_L = 4{\cdot}952 \cdot 10^{-5}$M.

With a decreasing excess metal concentration, the splitting of the two absorption bands becomes less pronounced and finally completely disappears (equimolar solutions). In solutions with excess ligand, the long-wavelength absorption band shifts to 625 nm and its long-wavelength side is perceptibly distorted. The other chelate bands are overlapped by the ligand absorption.

The optical characteristics of the blue Ni(II) chelate with TAMP are surveyed for various experimental conditions in Table II.

*The Absorbance–*pH *Curves*

All the measurements were performed using the special apparatus[28] described above. Each $A = f(\mathrm{pH})$ dependence for various concentration excesses was obtained from two or three independent measurements, the number of points in the region of equilibrium establishment always being greater than 20.

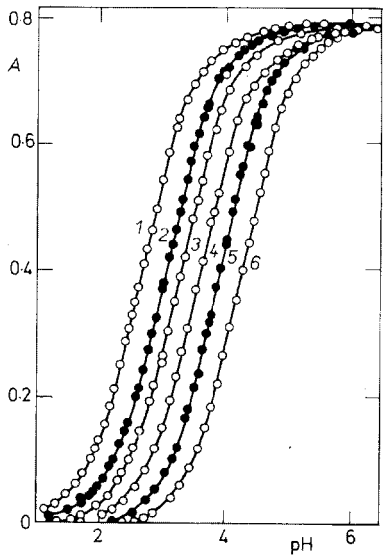

FIG. 4

The Absorbance–pH Curves of Ni(II) Solutions with TAMP for Various Excess Concentrations of Ni(II)

$c_L = 4{\cdot}952 \cdot 10^{-5}$M TAMP, $I = 0{\cdot}10$, 610 nm, for the other conditions see Fig. 3. Curve, c_M/c_L: *1* 250, *2* 100, *3* 50, *4* 25, *5* 10, *6* 5.

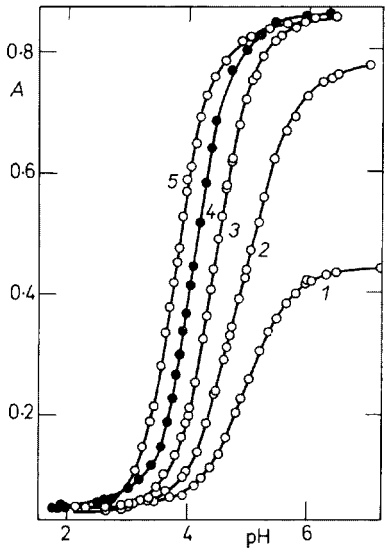

FIG. 5

The Absorbance–pH Curves of Ni(II) Solutions with TAMP for Excess Ligand Concentrations

$c_M = 2{\cdot}476 \cdot 10^{-5}$M, 610 nm, for the other conditions see Fig. 3. Curve, c_L/c_M: *1* 1, *2* 2, *3* 5, *4* 10, *5* 20.

The solution in the titration vessel, with concentrations c_M, c_L, I and 30% ethanol and with pH 1–3, was titrated with hydroxide solutions (c_{OH} = 2M, 0·05M and 0·005M-NaOH) using three burettes. The concentrations of all solution components were maintained constant by adding equal volumes of a Ni^{2+} with TAMP solution with twice the component concentrations ($2c_M$, $2c_L$, 60% ethanol) and with pH about

TABLE III

The Elucidation of the Most Probable Mechanism of the TAMP Reaction with Ni(II) 610 nm, I = 0·10, t = 25·00°C, 30% vol. C_2H_5OH.

mqn	r_{xy} graph.	U anal.	r_{xy} log. anal.	*mqn*	r_{xy} graph.	U anal.	r_{xy} log. anal.
		c_M/c_L = 100				c_M/c_L = 50	
111	·99 447	·4 445 . 10^{-2}	·99 936	111	·99 743	·4 932 . 10^{-1}	·99 978
112	·16 615	·1 952 . 10^{1}	·27 049	112	·04 960	·7 518 . 10^{3}	·18 560
121	·53 596	·9 541 . 10^{5}	·80 860	121	·68 300	·7 892 . 10^{4}	·88 599
211	·99 447	·4 445 . 10^{-2}	·99 936	211	·99 743	·5 202 . 10^{-1}	·99 978
122	·52 061	·4 376 . 10^{0}	·20 438	122	·92 096	·6 403 . 10^{3}	·34 806
212	·16 607	·5 043 . 10^{3}	·27 084	212	·04 960	·1 228 . 10^{4}	·18 650
221	·53 596	·2 986 . 10^{5}	·80 860	221	·68 300	·1 918 . 10^{5}	·88 599
222	·52 061	·5 430 . 10^{3}	·27 084	222	·92 096	·1 414 . 10^{4}	·34 806
		10				1	
111	·99 760	·1 258 . 10^{-2}	·99 867	111	·59 414	·6 650 . 10^{0}	·57 370
112	·21 768	·8 261 . 10^{3}	·21 617	112	·69 624	·2 083 . 10^{1}	·99 493
121	·50 205	·9 912 . 10^{6}	·62 729	122	·99 264	·9 255 . 10^{-1}	·99 763
211	·99 760	·1 319 . 10^{-2}	·99 867	211	·52 923	·7 057 . 10^{2}	·85 733
122	·54 850	·1 562 . 10^{7}	·29 917	121	·97 325	·3 434 . 10^{8}	·91 146
221	·50 205	·1 725 . 10^{7}	·62 729	221	·62 778	·1 435 . 10^{6}	·79 949
212	·21 768	·9 108 . 10^{3}	·21 617	212	·29 575	·2 227 . 10^{1}	·51 954
222	·54 850	·3 285 . 10^{7}	·29 917	222	·68 329	·3 122 . 10^{4}	·70 981
		0·1				0·05	
111	·95 537	·1 621 . 10^{1}	·97 599	111	·98 805	·1 518 . 10^{1}	·99 783
112	·78 149	·2 974 . 10^{1}	·88 829	112	·72 593	·2 653 . 10^{1}	·78 912
121	·67 163	·9 291 . 10^{2}	·98 489	121	·65 439	·1 007 . 10^{3}	·76 893
211	·88 933	·3 177 . 10^{0}	·93 863				
122	·99 289	·1 155 . 10^{1}	·99 711	122	·99 398	·3 279 . 10^{1}	·99 514
212	·50 032	·1 081 . 10^{1}	·70 884	212	·52 385	·1 286 . 10^{1}	·74 396
221	·67 375	·6 754 . 10^{0}	·98 741				
222	·86 744	·5 006 . 10^{2}	·98 326	222	·98 898	·9 377 . 10^{1}	·85 155
133	·90 756	·6 847 . 10^{4}	·28 591	133	·80 292	·1 112 . 10^{6}	·83 288

3–4. The overall consumption of the hydroxide and thus also of the other solution did not exceed 2–5 ml, with an initial titrand volume of $v_0 = 75$ ml.

The blue Ni(II) chelate with TAMP is formed at pH ~ 1–2 in solutions with excess metal ion or ligand, while in equimolar solutions it is formed only at pH ~ 4. The shape of the $A = f(\text{pH})$ curves clearly indicates a single complexation equilibrium in all cases (the curves are symmetrical and shift to more acidic regions with increasing excesses of the given component).

At pH > 6·5, the ligand absorption plays a role in equimolar solutions and in solutions with excess ligand (the anionic form with a maximum at 565 nm and ε_{max} ~ ~ 16 000) and completely prevents precise measurement of absorbance in this acidity region under these concentration conditions (Figs 4, 5).

Graphical Interpretation

Graphical interpretation of the absorbance–pH curves was performed under complex formation conditions, when the ligand exists in the solution practically only in its molecular form, LH, with minute concentrations of the cationic form, LH_2^+, at lower pH values[14]. According to the general complexation equilibrium,

$$m\,M + n\,LH_x \rightleftharpoons M_mL_nH_{nx-q} + q\,H \qquad (A)$$

reaction schemes characterized by molar reaction coefficients m, q and n equal to 111, 122, 112, 211, 222 and 212 can be considered most probable; in some special cases, equilibria of the 121, 242 and 221 type can also be assumed, with simultaneous ligand dissociation

$$LH_2^+ \rightleftharpoons LH + H\,. \qquad (B)$$

Graphical representation of the slope-intercept transformations, $A = f(F_i)$ or $A = f(G_i)$, is depicted in Fig. 6 for the first six combinations of the m, q and n coefficients, for a hundred-fold excess of nickel(II) ions ($c_M = 100\,c_L = 4{\cdot}952 \cdot 10^{-3}$M) and for the chelate absorption maximum wavelength, λ_{max} 610 nm. It is evident that only the dependences for m, q and n values of 111 or 211 are linear. Analogous conclusions hold for other Ni(II) concentration excesses (c_M/c_L = 250, 100, 50, 25, 10 and 5) and for all the measured wavelengths (560, 580, 610, 630, 650 and 670 nm).

The $A = f(F_i)$ dependence for $m = n = q = 1$, for a wavelength of 610 nm and for various Ni(II) concentration excesses $c_M/c_L = 5-250$, is shown in Fig. 7. The straight line intercept and slope values change only slightly within the variation of the concentration ratios and of the wavelength. The number of protons liberated during metal bonding (coefficient q), $q = 1$, was further verified under the above concentration ratios by the results of the graphical logarithmic analysis of the $\log F = f(\text{pH})$ dependences (the average q values found is 0·99), see Fig. 8.

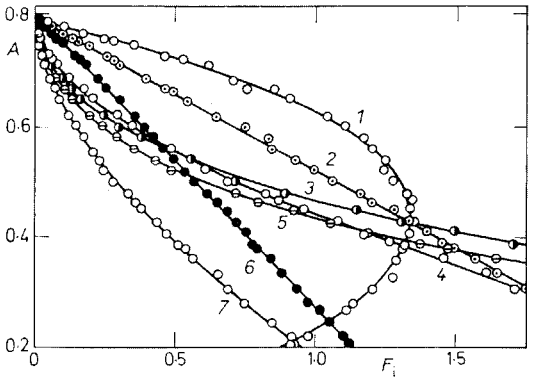

FIG. 6

Direct Graphical Analysis of the Absorbance–pH Curves for a Hundred-fold Ni(II) Concentration Excess and for the Individual Assumed Mechanisms

$c_M = 100\, c_L = 4{\cdot}952 \,.\, 10^{-3}$M, 610 nm, for the other conditions see Fig. 3. Curve-values of coefficients mqn — F_i-axis module: *1* 112 2 . 10^2, *2* 211 10^2, *3* 122 4 . 10^5, *4* 121 10^2, *5* 221 10^2, *6* 111 10^2, *7* 222 10^3. The order of reactions: $M + 2\,LH = ML_2H + H$, $2\,M + LH = M_2L + H$, $M + 2\,LH = ML_2 + 2\,H$, $M + LH_2 = ML + 2\,H$, $2\,M + LH_2 = M_2L + 2\,H$, $M + LH = ML + H$, $2\,M + 2\,LH = M_2L_2 + 2\,H$. For the definition of F_i see Table I.

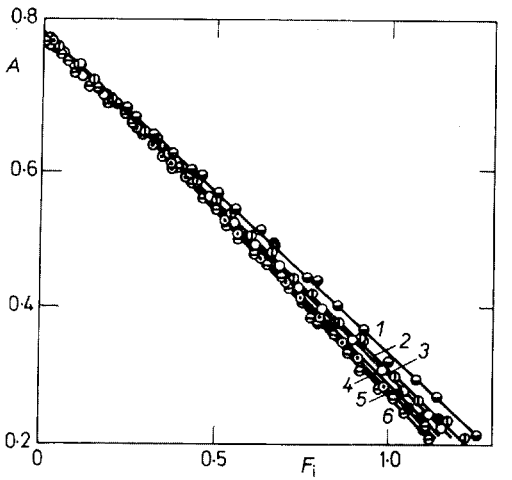

FIG. 7

Direct Graphical Analysis of the Absorbance–pH Curves for Various Ni(II) Concentration Excesses and the Reaction Mechanism, $M + LH = ML + H$

$c_L = 4{\cdot}952 \,.\, 10^{-5}$M, 610 nm, for the other conditions see Figs 3 and 4. Curve, c_M/c_L: *1* 5, *2* 10, *3* 50, *4* 25, *5* 250, *6* 100.

Minute deviations from linearity of the $\log F = f(\mathrm{pH})$ dependence in acidic media, $\mathrm{pH} < 1{\cdot}5-2{\cdot}0$, and the resulting change in the slope may be caused by the simultaneous equilibrium

$$\mathrm{Ni} + \mathrm{HL} \rightleftharpoons \mathrm{NiLH} \text{ or } \mathrm{Ni} + \mathrm{LH_2} \rightleftharpoons \mathrm{NiLH} + \mathrm{H} \qquad (C), (D)$$

in addition to the principal equilibrium

$$\mathrm{Ni} + \mathrm{HL} \rightleftharpoons \mathrm{NiL} + \mathrm{H}\,. \qquad (E)$$

The non-linearity of the dependence with lower metal concentration excesses and high pH values (curves 4–6, Fig. 8) can analogously be explained by a simultaneous side complexation equilibrium of the type

$$\mathrm{NiL} + \mathrm{LH} \leftrightharpoons \mathrm{NiL_2} + \mathrm{H}\,. \qquad (F)$$

The direct graphical analysis of the absorbance–pH curves for solutions with $c_M/c_L \geqq \geqq 10$ (without considering corrections for the complex-bound metal) does not differentiate formation of polynuclear complexes when the same number of protons is dissociated on complexation. Therefore the $\mathrm{pH}_{0i} = f(\log c_M)$ dependence was plotted for corresponding solutions; this dependence indicates that the presence of polynuclear complexes, $\mathrm{M_mL_n}$ with $m > 1$, can be excluded, since the slope, m/q, is approximately unity for the whole given concentration range and for pH values from 1·5 to 6·0 (Fig. 9).

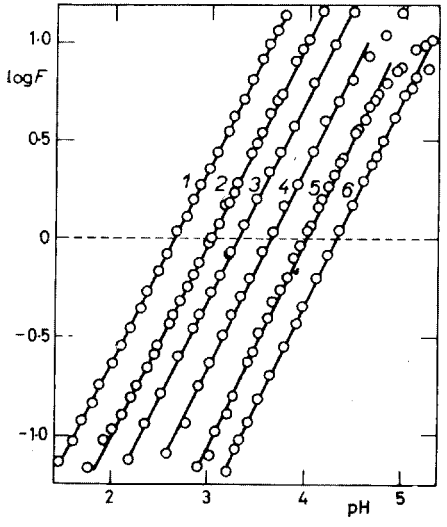

FIG. 8

Graphical-logarithmic Analysis of the Absorbance–pH Curves for Various Ni(II) Concentration Excesses

For the reaction conditions see Figs 3 and 4. Curve, c_M/c_L: *1* 250, *2* 100, *3* 50, *4* 25, *5* 10, *6* 5.

In equimolar solutions and in solutions with excess ligand, a mixture of two complexes is formed. The absorbance values on the horizontal parts of the absorbance–pH curves are roughly twice as high as those for the identical analytical concentrations of the minor component indicating that some higher complex is formed, M_mL_n with $n > 1$. For this reason, in addition to the above equilibria, equilibria between two complexes were also considered during the graphical data interpetation,

$$ML + LH \rightleftharpoons ML_2H \qquad (G)$$

neglecting the complex-bound metal and ligand concentrations and introducing a correction for the absorption of the ligand, $\Delta A = A - A_L$. Several approximations were required in order to determine the molar absorption coefficients of the two particles in solution.

Only the dependence for *mqn* values equal 112 is linear. The results of the graphical-logarithmic analysis lead to the same conclusions.

Interpretation Using the PRCEK Program

The absorbance–pH curves were interpeted by the linear least squares method using relations for the slope-intercept transformations, $A = f(F_i)$, $A = f(G_i)$ and $\log F = f(\mathrm{pH})$, analogous to those given in Table I.

The most probable reaction mechanism for the complex formation was selected only for 610 nm and concentration ratios of c_M/c_L = 100, 50, 10, 1 and 0·1, under assumptions identical to those made for graphical data interpretation. All the above

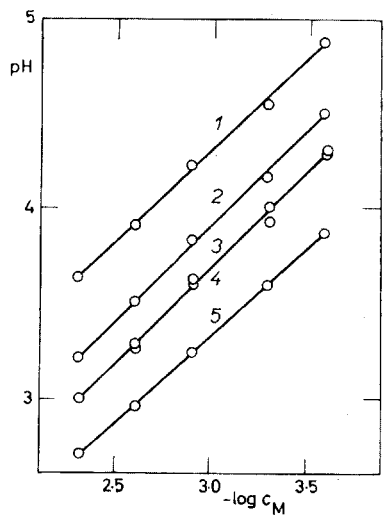

FIG. 9

The $pH_{oi} = f(\log c_M)$ Plot for Corresponding Solutions in the Ni(II)–TAMP Systems and the Conditions Specified for Fig. 8

Curve, *A*: *1* 0·650, *2* 0·500, *3* log $F = 0$, *4* 0·400, *5* 0·250.

mqn coefficient combinations were considered. On the basis of the criterion chosen (*i.e.* the correlation coefficient value and the sum of the squares of the deviations, r_{xy} and U, respectively), the conclusions drawn from the graphical curve interpetation were confirmed; it can be concluded that the ML complex is formed in solutions with higher metal ion concentration excesses, since the lowest sum of the squares of the deviations ($U \sim 10^{-3}$) and correlation coefficient values closest to unity ($r_{xy} \sim 0{\cdot}98$) were found for coefficient *mqn* values of 111 and 211 (Table III).

Curves $A = f(\mathrm{pH})$ were calculated for the given reaction mechanism for the formation of complex ML (reaction E), for all metal ion concentration excesses, $c_M/c_L \geqq \geqq 5$ and for all measured wavelengths. The results of the direct and logarithmic analysis of the absorbance–pH curves, obtained by the PRCEK program after the required number of iterations, are given in Table IV for various concentration excesses and wavelengths.

Good agreement among the results is evident in the concentration interval, $c_M = 5 \cdot 10^{-4} - 1{\cdot}25 \cdot 10^{-2}$M. For $c_M = 2{\cdot}476 \cdot 10^{-4}$M and a five-fold excess of Ni(II) the deviations are somewhat higher, indicating that some other complexation equilibrium takes place.

In addition, equilibria (F) and (G) were again considered for equimolar solutions and solutions with excess ligand. With equimolar solutions, the correlation coefficient values and the sums of the squares of the deviations never reached the values ($r_{xy} > 0{\cdot}99$, $U < 10^{-2}$) required to verify linearity of the $A = f(F_i)$ and $A = f(G_i)$ dependences. The best agreement was achieved for $mqn = 122$, *i.e.* complex ML_2. Analogous conclusions can be drawn for solutions with excess ligand, $c_L/c_M = 10$.

On the basis of these results, all the absorbance-pH curves with c_L/c_M ratios of 1, 2, 5, 10 and 20 and for wavelengths of 560, 570, 580, 600, 630, 650 and 670 nm were then treated for $mqn = 122$ with the full number of iterations. Some results are given in Table IV. The results again confirm the existence of a mixture of complexes NiL^+ and NiL_2 in equimolar solutions and in solutions with a small ligand excess, while complex NiL_2 is preferentially formed in solutions with higher ligand concentration excesses, $c_L/c_M \geqq 10$.

Data Interpretation Using the LETAGROP SPEFO Program

On the basis of the composition of the complexes determined by the graphical methods, the assumed complexes were described by the general formula $(Ni)_m(-H)_q \cdot (LH)_n$ with the corresponding equilibrium constant, $K_{mqn} = [(M)_m(-H)_q(LH)_n] \cdot [H]^q[M]^{-m}[LH]^{-n}$.

In order to decrease the consumption of computer time during treating data (c. 2000 experimental points), the whole set of the experimental values was separated into two independent parts on the basis of the above results:

a) solutions with metal ion concentration excess, $c_M/c_L \geqq 5$
b) equimolar solutions and solutions with ligand excess.

As the input values of the molar absorption coefficients for various wavelengths and of the complex equilibrium constants, those obtained by graphical analysis were used. The same was followed with the corresponding values for the metal and the ligand alone.

Complexes NiL (111), NiL_2 (121), NiLH (101) and NiL_2H (112) in the presence of various acidobasic ligand forms, LH_2^+ (−011), LH (001) and L^- (011), were gradually considered. The values in parentheses are the *mqn* coefficients in the formula, $(Ni)_m(-H)_q(LH)_n$.

After separate treatment of the above two parts of the whole data set (series 1–5 and 6–9), the whole set was solved together using the results of series 5 and 9 as the input values for the complex equilibrium constants and their molar absorption coefficients. Some of the results obtained are given in Tables V and VI.

Comparing the sum of the squares of the deviations, U, and the corresponding standard deviations of the absorbance, $\sigma(A)$, the best values were obtained with series 5 for solutions with excess Ni(II) and with series 9 for the other case. In the calculation of the whole set, the best agreement was obtained with series 11, assuming that complexes ML, MLH, ML_2 and ML_2H exist simultaneously. Therefore two more protonated complexes which were not detected by the graphical methods and

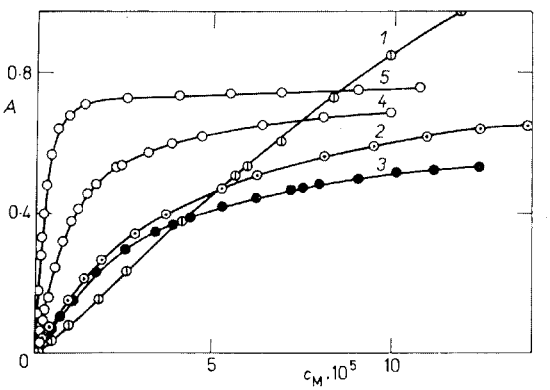

FIG. 10

The Curves of the Absorbance Dependence on the Component Concentration, $A = f(c_M)$ at a Constant Solution pH

Curve: *1* $c_L = 9{\cdot}904 \cdot 10^{-5}$M, pH 2·10, *2* $c_L = 4{\cdot}952 \cdot 10^{-5}$M, pH 3·50, module $A = 2$, *3* $c_L = 4{\cdot}952 \cdot 10^{-5}$M, pH 4·00, module $A = 1$, *4* $c_L = 4{\cdot}952 \cdot 10^{-5}$M, pH 5·20, module $A = 1$, *5* $c_L = 4{\cdot}952 \cdot 10^{-5}$M, pH 5·50, module $A = 1$.

TABLE IV

A Survey of the Values of the Molar Absorption Coefficients and Equilibrium Constants K_{111} and K_{122} for Various Concentration Conditions, Obtained by Direct Reading ($\varepsilon = A_{02}/c_i$), by Graphical Methods and Using the PRCEK II Program

λ	ε direct	$-\log K$ direct	ε graphical	$-\log K$ graphical	tg α	r_{xy}	$\varepsilon \pm d(\varepsilon)$		$-\log K$ PRCEK II	$10^2 U$	r_{xy}	$-\log K$	tg α
							$p_M = 250$						
560	11 260	0·73	11 560	0·73	0·73	1·04	·9 995	11 791 ±	174 0·7 347 ± 0·0 627	·5 022	·9 976	0·7 344 ±	0·0 154 ·9 943
580	14 240	0·72	14 420	0·72	0·71	·99	·9 975	14 251	26 0·7 452 0·0 705	·0 581	·9 997	0·7 361	0·0 324 ·9 954
610	16 050	0·70	16 505	0·73	0·73	·99	·9 968	16 147	27 0·7 387 0·0 672	·1 235	·9 996	0·7 431	0·0 148 ·9 911
630	14 870	0·70	15 000	0·73	0·74	1·00	·9 980	14 230	119 0·7 450 0·0 877	·0 745	·9 996	0·7 227	0·0 597 ·9 884
650	13 500	0·72	13 820	0·73	0·72	·99	·9 993	13 673	57 0·7 447 0·0 901	·0 311	·9 991	0·7 414	0·0 502 ·9 851
670	9 500	0·71	9 805	0·73	0·72	·98	·9 987	9 372	20 0·7 047 0·0 509	·2 730	·9 990	0·7 415	0·0 392 ·9 862
∅		0·71		0·73	0·72	·99	·9 983		0·7 405 0·0 715		·9 991	0·7 365	0·0 352 ·9 901
							$p_M = 100$						
560	11 330	0·73	11 510	0·74	0·72	·98	·9 990	11 448	12 0·7 280 ·0 609	·0 336	·9 995	0·7 279	·0 156 ·9 815
580	14 095	0·73	14 360	0·73	0·71	·99	·9 977	14 082	16 0·7 449 ·0 535	·0 644	·9 996	0·7 156	·0 068 ·9 959
610	16 135	0·74	16 480	0·72	0·71	·98	·9 967	16 181	24 0·7 470 ·0 698	·1 404	·9 995	0·7 162	·0 133 ·9 895
630	14 700	0·75	14 985	0·75	0·73	·98	·9 974	14 872	22 0·7 502 ·0 897	·1 087	·9 997	0·7 480	·0 207 ·9 935
650	13 330	0·73	13 530	0·73	0·73	·99	·9 996	13 390	9 0·7 402 ·0 329	·0 179	·9 990	0·7 385	·0 124 1·007
670	9 490	0·74	9 550	0·73	0·73	·99	·9 991	9 475	9 0·7 389 ·0 512	·0 165	·9 997	0·7 394	·0 056 ·9 930
∅		0·73		0·73	0·72	·98	·9 983		0·7 415 ·0 596		·9 995	0·7 309	·0 124 ·9 930
							$p_M = 50$						
560	11 320	0·72	11 470	0·72	0·74	·99	·9 975	11 192	35 0·7 326 ·0 823	·0 664	·9 993	0·7 262	·0 145 1·017
580	14 015	0·73	14 420	0·72	0·73	·99	·9 973	13 858	47 0·7 323 ·0 899	·1 148	·9 993	0·7 301	·0 268 1·007
610	16 015	0·73	16 460	0·72	0·73	·99	·9 984	16 230	34 0·7 368 ·0 711	·0 582	·9 989	0·7 320	·0 202 ·9 853
630	14 700	0·74	15 105	0·74	0·74	·99	·9 983	14 856	27 0·7 298 ·0 633	·0 350	·9 998	0·7 286	·0 122 ·9 868

650	13 330	0·75	13 570	0·73	0·74	·97	·9 993	13 396	± 25	0·7 491	± ·0 652	·0 315	·9 998	0·7 391	± ·0 153	1·003	
670	9 390	0·74	9 610	0·72	0·73	·98	·9 993	9 398	28	0·7 317	·0 910	·0 405	·9 996	0·7 367	·0 197	1·004	
∅		0·73		0·72	0·73	·99	·9 984			0·7 354	·0 771		·9 996	0·7 321	·0 181	1·00	
							$p_M = 25$										
560	11 230	0·70	11 310	0·73	0·70	·98	·9 988	11 168	22	0·7 279	·0 794	·0 323	·9 991	0·7 320	·0 127	·9 909	
580	14 015	0·70	14 200	0·74	0·74	·99	·9 972	14 164	64	0·7 428	·0 896	·2 813	·9 984	0·7 347	·0 341	·9 890	
610	15 955	0·69	16 340	0·75	0·73	·99	·9 996	16 313	77	0·7 334	·0 843	·4 008	·9 985	0·7 199	·0 341	·9 941	
630	14 640	0·72	14 885	0·76	0·72	0·97	·8 989	15 027	106	0·7 267	·0 732	·7 513	·9 970	0·7 490	0·0 513	·9 965	
650	13 330	0·71	13 650	0·75	0·75	1·00	·9 964	13 655	60	0·7 412	·0 896	·2 449	·9 988	0·7 333	·0 398	·9 889	
670	9 350	0·71	9 570	0·75	0·71	0·99	·9 990	9 436	16	0.7 366	·0 746	·0 180	·9 998	0·7 375	·0 178	·9 915	
∅		0·71		0·75	0·72	0·99	·9 983			0·7 348	·0 818	·3 151	·9 986	0·7 344	·0 316	·9 918	
							$p_M = 10$										
560	11 170	0·69	11 470	0·72	0·67	0·99	·9 962	11 395	21	0·7 515	·0 710	2·586	·9 998	0·7 312	·0 172	1·001	
580	14 035	0·69	14 380	0·72	0·72	0·97	·9 938	14 660	78	0·7 327	·0 828	6·653	·9 968	0·7 330	·0 166	·9 969	
610	15 850	0·69	16 740	0·72	0·72	0·99	·9 977	16 469	80	0·7 255	·0 748	·9 401	·9 997	0·7 293	·0 312	·9 975	
630	14 580	0·68	14 690	0·73	0·71	0·99	·9 978	14 983	86	0·7 410	·0 650	·9 694	·9 989	0·7 334	·0 241	·9 892	
650	13 330	0·69	14 135	0·72	0·73	0·99	·9 972	13 487	88	0·7 435	·0 997	·7 980	·9 971	0·7 228	·0 215	·9 888	
670	9 690	0·69	9 875	0·73	0·68	0·99	·9 982	9 806	48	0·7 302	·0 977	2·979	·9 987	0·7 392	·0 196	·9 902	
∅		0·69		0·72	0·71	0·99	·9 968			0·7 357	·0 768	3·685	·9 985	0·7 324	·0 217	·9 939	
							$p_M = 5$										
560	11 120	0·70	11 390	0·74	0·72	0·99	·9 918	11 372	21	0·6 356	·0 610	1·258	·9 993	0·6 312	·0 159	·9 813	
580	14 035	0·67	14 350	0·73	0·69	0·98	·9 838	14 455	78	0·7 327	·0 688	1·605	·9 938	0·7 230	·0 399	·9 214	
610	15 850	0·72	16 405	0·75	0·73	0·99	·9 877	15 899	83	0·7 124	·2 168	1·910	·9 974	0·7 030	·0 380	·9 399	
630	14 665	0·71	15 000	0·74	0·70	1·00	·9 878	14 783	85	0·7 435	·2 774	1·909	·9 959	0·7 324	·0 357	·9 354	
650	13 340	0·69	13 770	0·75	0·71	0·99	·9 812	13 190	82	0·7 410	·3 231	1·749	·9 963	0·7 275	·0 373	·9 122	
670	9 390	0·70	10 140	0·74	0·72	0·99	·9 982	10 260	28	0·6 650	·0 978	2·242	·9 994	0·6 626	·0 266	·9 746	
∅		0·70		0·74	0·71	0·99	·9 884			0·7 051	·2 075	4·187	·9 970	0·6 967	·0 322	·9 441	

Table IV (continued) on the page 624.

TABLE IV
(*Continued*)

λ	ε direct	−log K	ε graphical	−log K	tg α	r_{xy}	ε ± d(ε) PRCEK II	−log K	$10^2 U$	r_{xy}	−log K	tg α
							mean values					
560	11 240	0·71	11 450	0·73	0·72	0·99	·9 964	11 394 ± 31	0·7 305 ± ·0 734[a]	4·232	·9 987	0·7 332[a] ± ·0 252	·9 938[a]
580	14 070		14 355					14 243 51	0·7 375[a]			0·7 272	
610	15 975		16 490					16 373 54					
630	14 665		14 945					14 891 74					
650	13 340		13 770					13 465 52					
670	9 480		9 760					9 634 25					
							$p_M = 0·5$					
560	18 100		18 920	0·62	0·58	1·2	·9 797	19 532 47	0·5 893	45·61	·9 989	0·2 744	·0 712 1·9 462
580	22 415		24 760	0·56	0·50	1·5	·9 388	26 252 72	0·4 888	3260	·9 878	0·3 640	·4 356 2·0 320
610	29 725		30 150	0·50	0·47	1·4	·9 496	31 906 104	0·5 111	2362	·9 906	0·3 604	·3 918 2·0 250
630	27 870		29 950	0·51	0·50	1·5	·9 725	31 300 63	0·4 154	5740	·9 916	0·3 729	·3 860 2·0 440
650	26 860		27 490	0·48	0·46	1·2	·9 836	27 867 77	0·5 043	3805	·9 994	0·3 381	·0 829 1·9 126
670	23 500		23 060	0·51	0·48	1·3	·9 830	23 021 84	0·4 125	3612	·9 991	0·3 389	·0 849 1·9 143
							$p_M = 0·2$					
560	19 180		23 540	0·67	0·68	1·9	·9 966	26 830 203	0·6 591	6·543	·9 966	0·6 049	·3 329 1·9 439
580	26 050		30 650	0·68	0·67	1·8	·9 970	32 886 360	0·7 038	18·62	·9 970	0·6 898	·4 665 2·0 000
610	33 320		34 870	0·70	0·69	1·7	·9 905	39 664 503	0·7 080	36·04	·9 959	0·6 353	·4 758 1·9 783
630	31 905		33 780	0·68	0·67	1·8	·9 933	37 137 394	0·6 898	22·19	·9 944	0·7 137	·4 553 2·0 100
650	29 280		30 175	0·69	0·71	1·9	·9 950	34 728 406	0·7 061	24·24	·9 977	0·6 936	·4 767 1·9 829
670	28 500		28 320	0·72	0·70	1·8	·9 932	28 494 354	0·7 071	17·83	·9 952	0·6 870	·3 811 1·9 901

						$p_M = 0{\cdot}1$						
560	19 380	20 150	0·78	0·81	1·9	·9 940	20 976 ± 140	0·8 542	27·43	·9 984	0·8 399 ±	·1 727 2·1 073
580	25 850	25 990	0·83	0·86	1·9	·9 942	26 106 760	0·8 537	2742	·9 974	0·8 417	·1 749 2·0 182
610	33 520	31 070	0·82	0·84	1·9	·9 928	30 150 928	0·8 502	11·11	·9 972	0·8 546	·1 770 2·0 280
630	31 905	30 480	0·83	0·83	1·9	·9 942	30 182 924	0·8 682	8·122	·9 977	0·8 394	·1 544 2·0 440
650	29 885	28 050	0·84	0·82	1·8	·9 950	27 672 755	0·8 663	53·88	·9 980	0·8 264	·1 653 2·0 384
670	28 600	24 355	0·80	0·81	1·9	·9 936	21 544 680	0·8 571	4·703	·9 975	0·7 969	·1 839 2·0 308
						$p_M = 0{\cdot}05$						
560	19 180	20 220	0·84	0·85	2·0	·9 889	21 031 278	0·8 785	7·068	·9 975	0·8 829	·0 461 1·9 270
580	26 050	26 605	0·84	0·84	1·9	·9 887	26 953 447	0·8 912	16·56	·9 975	0·8 845	·0 563 1·9 123
610	33 724	32 200	0·84	0·86	1·9	·9 878	33 372 588	0·8 910	28·93	·9 972	0·8 846	·0 556 1·9 188
630	31 905	31 000	0·84	0·82	1·9	·9 897	30 636 520	0·8 910	2·235	·9 980	0·8 811	·0 543 1·9 120
650	29 890	27 955	0·80	0·86	1·9	·9 857	27 763 491	0·8 900	1·291	·9 861	0·8 802	·0 548 1·9 148
670	28 600	24 265	0·86	0·89	1·9	·9 918	24 308 382	0·8 783	1·237	·9 961	0·8 782	·0 526 1·8 689

[a] Average of the values for $c_M/c_L > 5$, $p_M = c_M/c_L$

with the PRCEK program were found in the solution (with the required probability, 93·3%). Selected values of the molar absorption coefficients for the individual complexes and the ligand acidobasic forms are given in Table VI.

The Curves of the Absorbance Dependence on the Component Concentration

The absorbance *vs* concentration curves were measured (Fig. 10) for the dependence on the concentration of excess component at a constant concentration of the other component and a constant pH values, $A = f(c_{\text{comp 1}})$, for several suitably chosen pH values in the interval, pH 2–6. The measurement was again carried out using the above described apparatus, by titrating 25 ml of a solution in the titration vessel with

TABLE V

A Survey of the Values of the Sum of the Squares of the Deviations, $U_{\min}$, and of the Deviations of the Absorbance, $\sigma(A)$, for the Individual Computation Cycles, Obtained with the LETAGROP SPEFO Program

N_s	mqn[a]	$U_{\min}$	$\sigma(A)\ 10^3$	Conditions
1	011, 111, 0–11	$2{\cdot}1438 \cdot 10^{-1}$	17·64	$A = f(\text{pH}),\ c_M/c_L \geqq 5$
2	011, 111,	$1{\cdot}1818 \cdot 10^{-1}$	13·10	$A = f(\text{pH}),\ c_M/c_L \geqq 5$
3	011, 111, 122	$4{\cdot}4471 \cdot 10^{-2}$	8·14	$A = f(\text{pH}),\ c_M/c_L \geqq 5$
4	011, 111, 122, 101	$3{\cdot}7613 \cdot 10^{-2}$	7·46	$A = f(\text{pH}),\ c_M/c_L \geqq 5$
5	011, 111, 122, 101, 112	$3{\cdot}6249 \cdot 10^{-2}$	7·35	$A = f(\text{pH}),\ c_M/c_L \geqq 5$
6	011, 111	2·1969	54·20	$A = f(\text{pH}),\ c_L/c_M \geqq 1$
7	011, 111, 122	$3{\cdot}7586 \cdot 10^{-1}$	22·97	$A = f(\text{pH}),\ c_L/c_M \geqq 1$
8	011, 111, 122, 112,	$3{\cdot}2072 \cdot 10^{-1}$	20·90	$A = f(\text{pH}),\ c_L/c_M \geqq 1$
9	011, 111, 122, 112, 101	$1{\cdot}8557 \cdot 10^{-1}$	14·10	$A = f(\text{pH}),\ c_L/c_M \geqq 1$
10	011, 111, 122	$2{\cdot}6195 \cdot 10^{-1}$	27·32	$A = f(\text{pH}),\ c_M/c_L \leqq 250$
11	011, 111, 122, 112, 101	$7{\cdot}6919 \cdot 10^{-2}$	23·13	
12	111, 201, 101	$9{\cdot}4017 \cdot 10^{-4}$	4·52	$A = f(c_M),\ \text{pH} < 4$
13	111, 122, 101, 112	$3{\cdot}5658 \cdot 10^{-2}$	7·31	$A = f(c_M),\ \text{pH} > 5$
14	111, 201, 211	$1{\cdot}9621 \cdot 10^{-2}$	16·90	$A = f(c_M),\ \text{pH} < 2$
15	111, 122, 101	$1{\cdot}6716 \cdot 10^{-2}$	19·41	$A = f(c_M),\ \text{pH} < 2$
16	111, 122, 101, 112	$1{\cdot}6104 \cdot 10^{-1}$	14·88	$A = f(c_L),\ \text{pH} > 4$
17	111, 122, 101, 201	$6{\cdot}3233 \cdot 10^{-4}$	4·09	$A = f(c_M, c_L),\ \text{pH} > 1$

[a] 0–11 LH_2^+, 011 L^-, 111 ML, 122 ML_2, 101 MLH, 112 ML_2H, 201 M_2LH.

component concentrations, c_{L0} and $c_{M0} \to 0$ or $c_{L0} \to 0$ and c_{M0}, with solutions of components concentrations $c_{L1} = c_{L0}$ and $c_{M1} \gg c_{M0}$ or $c_{L1} \gg c_{L0}$ and $c_{M1} = c_{M0}$, using two burettes. One of the titrants has a pH identical with that of the titrand, the other had a pH 0·5 unit higher. The latter solution compensated possible acidity changes in the measured solution. The concentration of the variable component was

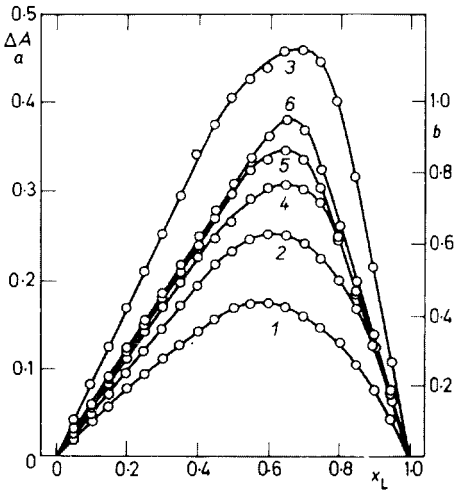

FIG. 11

The Continuous Variation Curves for Ni(II) Solutions with TAMP

$c_0 = c_L + c_M = 9{\cdot}904 \,.\, 10^{-5}$M, 610 nm. Curve pH *A*-axis module: *1* 4·00 *a*/2, *2* 4·50 *a*, *3* 5·00 *b*/2, *4* 5·50 *b*, *5* 6·00 *b*, *6* 7·00 *b*.

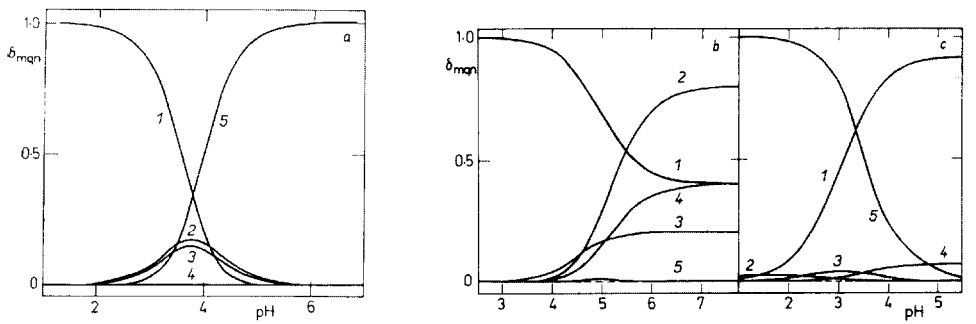

FIG. 12

The Distribution Diagrams for the Ni(II) System with TAMP in a 30% Ethanol Medium, $\delta_{mqn} = f(\text{pH})$

The reaction equilibrium constant values are given in Table VIII *a*) Curves for ligand concentration excess $c_L = 20\, c_M = 4{\cdot}952 \,.\, 10^{-5}$M, $\delta_{mqn} = n[M_mL_nH_{nx-q}]/c_M$. Curve, complex: *1* M, *2* ML, *3* ML_2H, *4* MLH, *5* ML_2; *b*) Equimolar solutions $c_M = c_L = 2{\cdot}476 \,.\, 10^{-5}$M . $\delta_{mqn} = n[M_mL_nH_{nx-q}]/c_M$, *1* LH, *2* ML_2, *3* ML, *4* ML_2 — $\delta_{mqn} = [ML_2]/c_L$, *5* ML_2H, [MLH] ~ 0; *c*) One hundred-fold concentration excess of Ni(II), $c_M = 100\, c_L$, $\delta_{ij} = m[M_m \,.\, L_nH_{nx-q}]/c_L$, *1* ML, *2* MLH, *3* ML_2H, *4* ML_2, *5* HL.

TABLE VI

The Molar Absorption Coefficients from Some Computation Cycles, Obtained Using the LETAGROP SPEFO Program

Species	560 nm		580 nm		610 nm		630 nm		650 nm		670 nm		$-\log K_{mqn}$	
						$N_s = 5$								
LH	453 ±	44	11 ±	47	0 ±	52	0 ±	51	0 ±	37	0 ±	41		
ML	11 605	47	14 275	51	16 261	50	14 497	53	13 271	38	9 231	42	0·7 447 ±	0·0 099
ML_2	17 547	1 104	21 781	1 179	26 463	1 017	30 034	1 087	27 003	786	21 352	850	0·8 089	0·0 683
MLH	2 346	4 197	2 105	4 483	0	4 939	0	5 091	0	3 516	0	3 901	−0·5 442	0·9 251[a]
ML_2H	0	5 873	0	5 297	0	5 095	0	5 003	0	4 952	0	4 892	−2·4 559	·9 789[a]
						$N_s = 9$								
LH	339	20	0	23	0	23	0	23	0	20	0	23		
ML	16 744	468	20 150	418	23 419	506	22 718	503	21 479	440	17 209	491	0·7 286 ±	0·0 477
ML_2	22 265	59	27 503	53	33 318	43	31 987	42	28 675	37	23 302	41	0·8 920	0·0 627
MLH	5 988	336	4 592	176	2 309	213	2 162	211	2 016	185	1 933	207	−0·9 382	0·0 455
ML_2H	0	5 278	0	3 151	0	3 806	0	3 782	0	3 308	0	3 695	−2·5 214	0·1 747
						$N_s = 11^{bd}$								
ML	11 605	47	14 275	51	16 261	50	14 497	53	13 271	38	9 231	42	0·7 392 ±	0·0 234
ML_2	22 265	59	27 503	53	33 318	43	31 987	42	28 675	37	23 302	41	0·8 388	0·0 282
MLH	5 988	336	4 592	176	2 309	213	2 162	211	2 016	185	1 933	207	−0·6 404	0·3 498
ML_2H	0		0		0		0		0		0		−2·4 958	1·1 488
						$N_s = 13^c$								
ML	11 522	98	14 252	105	16 267	116	14 777	127	13 440	95	9 334	100	0·7 426 ±	0·1 416
ML_2	19 038	1 033	22 536	1 103	25 697	1 202	24 005	1 313	22 713	987	16 956	1 041	0·8 839	0·1 429

$N_s = 16$

ML	16 263	± 530	18 957	± 493	21 851	± 504	21 309	± 127	20 305	± 463	16 247	± 551	0·3 587	± 0·0 809
ML_2	21 976	316	27 308	299	33 076	330	31 752	345	28 511	303	23 148	361	0·8 915	0·0 786
MLH	4 742	268	3 930	253	2 028	166	1 900	174	1 782	153	1 707	182	−0·6 283	0·1 971
ML_2H	57 178	2 719	68 621	2 565	80 833	1 788	75 218	1 817	67 339	1 644	56 505	1 957	−2·9 394	3·256[a]

$N_s = 17$[b]

ML	0·7 236	± 0·0 626
ML_2	0·8 874	0·2 760
MLH	−0·6 564	0·0 692
ML_2H	−2·5 523	0·0 127

[a] The maximum value, [b] the molar absorption coefficient values were not printed out, [c] the values for species MLH, ML_2H and M_2LH are not given, because of their poor reliability, [d] the molar absorption coefficient values from the preceding computation cycles are given.

calculated using the relation

$$c_i = c_{i0}(v_1 + v_2)/(v_0 + v_1 + v_2), \qquad (9)$$

where v_0, v_1 and v_2 are the solution volumes in the titration vessel and in the first and second burette, respectively, and c_i and c_{i0} are the resultant concentrations of the variable component and in the titration vessel at the beginning of the measurement, respectively.

Graphical analysis of the $A = f(c_L)$ or $A = f(c_M)$ curves (Fig. 10) was carried out using the printed-out values of variables F_i, G_i or Q_i after the first computation *cycle* (the PRCEK program). The curves were further analyzed employing the PRCEK program using the equations given in Table I and equations (5) and (6) in one computation cycle, and finally by the LETAGROP SPEFO program.

The criteria for various assumed stoichiometric ratios in the complexes (U, σA, r_{xy}), calculated according to the PRCEK and LETAGROP SPEFO programs, are compared for some of the measured curves in Tables VI and VII.

The results show that only the mononuclear complex, ML, is formed in solutions with excess metal ion ($A = f(c_M)$). The results for the $A = f(c_L)$ curves do not lead to unambiguous conclusions, since complex ML predominates over small concentrations of complex ML_2 at lower pH values, while at higher pH values complex ML_2 predominates. The handling of the curves with the help of the LETAGROP SPEFO program leads to the same results as the interpretation of the absorbance–pH curves and the obtained values of the molar absorption coefficients and the equilibrium constants are practically identical. The small disproportions in values at extreme

TABLE VII

The Molar Absorption Coefficient and the Equilibrium Constant Values, Obtained with the PRCEK II Program for the Curves of the Absorbance Dependence on the Component Concentrations 610 nm

Conditions, pH	$c_{const.}$	Direct analysis		$-\log K$	Logarithmic analysis
		r_{xy}	ε_2		$-\log K$ slope
$A = f(c_M)$, 3·50	$9{\cdot}904 \cdot 10^{-5}$M	·9892	13 530 ± 5 046	0·7149 ± 0·0059	0·6792 1·010
$A = f(c_M)$, 4·00	$4{\cdot}952 \cdot 10^{-5}$M	·9775	11 106 ± 4 922	0·6177 ± 0·0165	0·7982 1·367
$A = f(c_M)$, 5·20	$4{\cdot}952 \cdot 10^{-5}$M	·9557	14 539 ± 4 399	0·5745 ± 0·0074	0·6834 1·301
$A = f(c_M)$, 5·50	$4{\cdot}952 \cdot 10^{-5}$M	·8796	16 049 ± 833	0·5678 ± 0·0133	0·8965 1·388
$A = f(c_L)$, 5·20	$2{\cdot}476 \cdot 10^{-5}$M	·9427	35 254 ± 4 343	0·8893 ± 0·0209	0·8642 2·261
$A = f(c_L)$, 5·75	$2{\cdot}476 \cdot 10^{-5}$M	·9504	26 673 ± 949	0·8623 ± 0·0153	0·8438 1·661

TABLE VIII

Summarizing Values of the Molar Absorption Coefficient and Equilibrium Constant in the Ni(II)–TAMP System (30% Ethanol Medium)

Value	Method			
	direct	graphical	PRCEK II	LETAGROP SPEFO
			ML	
K		0·187	0·183 ± 0·004	0·182 ± 0·003
$-\log K^a$	0·696	0·735	0·730 ± 0·073	0·739 ± 0·024
$-\log K^b$		0·705	0·733 ± 0·025	
$\log \beta_{11}$		7·6	7·60 ± 0·05	7·595 ± 0·02
ε_{560}	11 240	11 450	11 390 ± 31	11 605 ± 47
ε_{580}	14 070	14 355	14 240 ± 51	14 275 ± 51
ε_{610}	16 490	15 975	16 370 ± 54	16 260 ± 50
ε_{630}	14 665	14 945	14 890 ± 74	14 500 ± 53
ε_{650}	13 770	13 340	13 465 ± 52	13 270 ± 38
ε_{670}	9 760	9 480	9 620 ± 25	9 230 ± 42
			ML_2	
K		0·13	0·130 ± 0·030	0·128 ± 0·004
$-\log K^a$		0·84	0·850 ± 0·062	0·839 ± 0·028
$-\log K^b$		0·85	0·882 ± 0·053	
$\log \beta_{12}$		15·81	15·805 ± 0·05	15·815 ± 0·03
ε_{560}	19 280	20 220	21 030 ± 278	22 265 ± 59
ε_{580}	26 050	26 605	26 955 ± 447	27 500 ± 53
ε_{610}	33 725	32 300	32 370 ± 588	33 320 ± 43
ε_{630}	31 905	31 000	30 635 ± 520	31 990 ± 42
ε_{650}	29 980	27 955	27 760 ± 491	28 675 ± 37
ε_{670}	28 600	24 265	24 310 ± 382	23 300 ± 41
			MLH^c	
K				4·8 ± 0·5
$\log K$				0·65 ± 0·35
			ML_2H^c	
K^c				(3·3 ± 0·5) . 10^2
$\log K$				2·5 ± 1·3

[a] Direct graphical analysis, [b] logarithmic-graphical analysis, [c] the molar absorption coefficient values are not given because of their low importance. The values in Table VI are only orientative. $\beta_{mn} = K_{mqn}/K_{a2}^n$

acidity conditions are probably caused by the low concentrations of the individual complexes; this also leads to poor precision of the determination of characteristic quantities for the complexes.

Analysis of the Continuous Variation Curves

The continuous variation curves, $Y = f(x_L)$, were obtained as follows: short absorbance–pH curves, $A = f(\mathrm{pH})$, were measured for individual values of the mole fraction, $x_L = c_L/c_0 = c_L/(c_L + c_M)$, in an analogous manner to that employed with the absorbance–pH curves, and the absorbances for the given pH values were obtained by graphical interpolation. The absorbances were corrected for the absorbances of the components alone and the expression $Y = A - A_{0L} - A_{0M} = f(x_L)$ was plotted.

The continuous variation curves also confirm the existence of a mixture of complexes with molar ratios M : L – 1 : 1 and 1 : 2 at lower pH values and of a complex with M : L = 1 : 2 at pH's above 5. The non-symmetry of curves for $x_L > 0{\cdot}5$ (see curves *3* and *5* in Fig. 11) indicates the presence of two complexes in the solution.

Distribution Diagrams for the Existence of the Complexes

On the basis of the calculated equilibrium constants of the complexes (Table VIII), the distribution existence diagrams, $\delta_{mqn} = f(\mathrm{pH})$, for complexes MLH, MLLH, ML_2 and ML and the acid–base species of the ligand, LH, were calculated for three different concentration ratios, $c_M/c_L = 100$, $c_M = c_L$ and $c_L/c_M = 10$, using the Minsk 22 computer and the HALTAFALL program (Fig. 12).

It is clear from the distribution diagram why it was impossible to obtain adequate results for solutions with small concentration excesses of one component or equimolar solutions, using the graphical interpretation of the absorbance curves. Here, in addition to small concentrations of complexes MLH and ML_2H, complexes ML and ML_2 coexist in the entire pH range. For example, 20% of complex ML and 78% complex ML_2 co-exist at pH 6–7.

At pH 3–4, complex ML is dominantly formed and complex ML_2 predominates at pH > 4·8 only. The poorer agreement of the results for solutions with excess ligand can be explained analogously. Complex ML predominates at pH = 2·0 to 3·3 and only at pH > 3·5 is the concentration of ML_2 higher; in solutions with excess nickel(II) ion, the concentration of complex ML is only negligibly affected by the concentrations of the other complexes in the entire pH range and hence the interpretation gives excellent results.

Similarly, the poor precision of results for characteristic parameters coming from the LETAGROP SPEFO program for complex ML in solutions with excess ligand, or for complex ML_2 in solutions with excess metal ion and for the two remaining

complexes under any conditions can be explained: similarly the concentrations of the particular complexes are then small, leading to large errors in the determination of the molar absorption coefficients and the equilibrium constants.

REFERENCES

1. Kawase A.: Bunseki Kagaku *11*, 621, 628 (1962).
2. Kawase A.: Bunseki Kagaku *12*, 817, 820, 903 (1963).
3. Kawase A.: Bunseki Kagaku *13*, 553 (1964).
4. Yanagihara T., Matano N., Kawase A.: Trans. Natl. Res. Inst. Metals *1*, 65 (1959).
5. Yanagihara T., Matano N., Kawase A.: Trans. Natl. Res. Inst. Metals *2*, 51, 56, 60 (1960).
6. Matano N., Kawase A.: Trans. Natl. Res. Inst. Metals *4*, 30 (1962).
7. Chromý V., Vřešťál J.: Chem. listy *60*, 1537 (1966).
8. Chromý V., Sommer L.: Talanta *14*, 393 (1967).
9. Sommer L., Šepel T., Ivanov V. M.: Talanta *15*, 949 (1968).
10. Kai F.: Anal. Chim. Acta *44*, 242 (1969).
11. Langová M., Havel J., Sommer L.: Chem. Anal. (Warsaw) *17*, 989 (1972).
12. Langová M., Machálková D., Sommer L.: Scripta Fac. Sci. Nat. Univ. Brunensis, Chemica 2, *2*, 229 (1972).
13. Chromý V., Sommer L.: Publ. Fac. Sci. Nat. Univ. Brunensis No *517*, 407 (1970).
14. Kubáň V., Havel J.: Acta Chem. Scand. *27*, 528 (1973).
15. Sommer L., Kučerová J., Procházková H., Hniličková M.: Publ. Fac. Sci. Nat. Univ. Brunensis, No *464*, 249 (1965).
16. Sommer L., Kubáň V., Havel J.: Folia Fac. Rerum Nat. Univ. Brno *11*, Chemia 7, Part 1, (1970).
17. Sommer L., Kubáň V.: This Journal *32*, 4355 (1967).
18. Chiacchierini E., Cocchieri R., Sommer L.: This Journal *38*, 1478 (1973).
19. Havel J., Kubáň V.: Scripta Fac. Sci. Nat. Univ. Brunensis, Chemia 2, *1*, 87 (1971).
20. Kubáň V.: Scripta Fac. Sci. Nat. Univ. Brunensis, Chemia 2, *2*, 81 (1972).
21. Sillén L. G., Warnqvist B.: Acta Chem. Scand. *22*, 3032 (1968).
22. Sillén L. G., Warnqvist B.: Arkiv Kemi *31*, 377 (1969).
23. Ingri N., Kakolowicz W., Sillén L. G., Warnqvist B.: Talanta *14*, 1261 (1967),
24. Elgqvist B.: Talanta *16*, 1502 (1969).
25. Havel J., Kubáň V.: Scripta Fac. Sci. Nat. Univ. Brunensis, Chemia 2, *2*, 95 (1972).
26. Svoboda V., Bendová L.: Unpublished results.
27. Toul J., Mouková N.: J. Chromatog. *67*, 335 (1972).
28. Kubáň V.: *Thesis*. University Brno 1972.
29. Asmus E.: Z. Anal. Chem. *195*, 244 (1963).
30. Klausen K. S., Langmyhr F. J.: Anal. Chim. Acta *28*, 325 ,501 (1963).
31. Job P.: Ann. Chim. (Paris) (10), *9*, 113 (1928); (11), *6*, 97 (1936).
32. Ostromyslenskii I.: Ber. *44*, 268 (1911).
33. Vosburg W. C., Cooper B. R.: J. Am. Chem. Soc. *63*, 427 (1941).

Translated by M. Štulíková.